

A 5G Camouflage Antenna for Pico-Cell Base Stations

Ahmed Alieldin¹, Yi Huang^{*1}, Manoj Stanley², Qian Xu³

¹ Department of Electrical Engineering and Electronics, the University of Liverpool, Liverpool, L69 3GJ, U.K

² National Physical Laboratory, Hampton Rd, Teddington TW11 0LW, UK.

³ College of Electronics and Information Engineering, Nanjing University of Aeronautics and Astronautics, Nanjing, China.

* yi.huang@liverpool.ac.uk

Abstract: A camouflage dual-polarized antenna for 5G pico-cell base stations is proposed in this paper. The antenna offers good coverage for the 5G sub-6 GHz frequency band (3.3-3.8 GHz) with a reflection coefficient better than -15 dB and a port-to-port coupling less than -23 dB. The proposed antenna consists of two layers (a radiating layer and a feeding layer) separated by an air gap. The radiating layer uses a transparent conducting film (Indium Tin Oxide) to form two patches (a radiating patch and a parasitic patch) printed on the opposite sides of a glass laminate. The radiating layer has visual transparency of 77%, which makes it possible to be integrated with the glass cover of the head of a street lamp while the feeding layer is embedded inside the head for camouflage. A 2×2 antenna array is formed to achieve a realized gain of 13.2 dBi and a 3-dB solid angle of $33^\circ \times 33^\circ$. Therefore, the proposed design is very suitable to be employed as a camouflage 5G pico-cell base station.

1. Introduction

To deliver that high-speed connectivity, the next generation of cellular networks (5G) will use new types or airwaves that do not travel far. Meaning carriers will need to build dense webs of small cell towers on the side of buildings, on lampposts, even on newspaper boxes, the cells are roughly the size of a laptop. Therefore, the small cell base stations are set to play an important role in expanding the capacity of wireless networks [1]. The design of pico-cell (PC) base stations has attracted the attention of the research and the industry communities as it has posed new challenges on making them small size, low power and low cost in comparison to the traditional Macrocell base stations [2].

To respond to the public pressure of less conspicuous antenna systems, designers tend to produce camouflage base station antennas, which can be visually hidden [3]. Two main approaches can be utilized to achieve the concept of constructing camouflage antennas. The first approach is to install the base station antenna on a customized platform that looks like a part of the surrounding environment, like a palm tree in a garden or a cactus tree on the side of a highway road as shown in Fig.1. This approach is quite costly as for the need of building a customized platform for each base station.



Fig.1. Base station antennas on camouflage platforms.

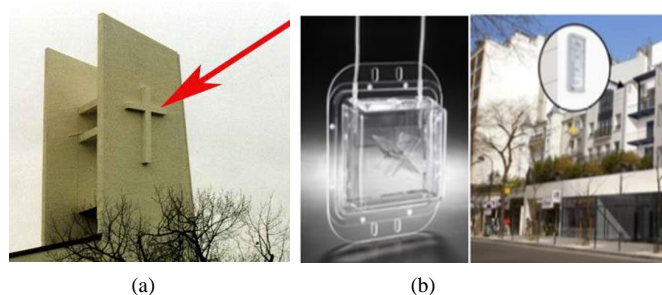


Fig.2. A camouflage base station integrated to (a) cathedral cross (b) window glass.

The second approach is to integrate the base station antenna to an already existing object in the surrounding environment such as the cross at the top of the cathedral shown in Fig.2(a), which is nothing but a base station antenna array or being integrated to the transparent window glass as shown in Fig.2(b).

The concept of using a camouflage antenna in wireless communication is nothing new. It has been adopted for both military [4] and civilian [5] applications. Furthermore, in [6], a transparent conductor printed on a glass substrate has been employed to form a transparent antenna, which is of low visibility and could be an attractive candidate for new PC base stations.

To make a transparent antenna, the selection of a suitable material is vital. Transparent conductive materials have been prepared with oxides of tin, indium, zinc and cadmium using magnetron sputtering [7]-[8]. These transparent conductive oxides (TCOs) are employed in a wide spectrum of applications such as solar cells, electromagnetic shielding and touch-panel controls [9]. Notably, there has been little commercial application of TCOs in antenna design. Attempts have been made to create transparent patch antennas for automobile windshields and solar cells [10]-[14].



Fig.3. The illustrative scenario of the 5G coverage area using the proposed PC base station.

Many papers on this subject expressed the inability to achieve high gains (larger than 2 dB) [13] due to the reduced efficiency of microstrip patch antennas with a ground plane compared with dipole antennas with no ground plane [12]. One of the problems is the skin depth losses introduced by the requirement of thin TCO depositions for high optical transparency. Furthermore, ground effect losses present in patch antennas further aggravate the loss due to skin effects. Both issues coupled with the relatively low conductivity of TCOs in comparison with copper [15], can cause significant increases in surface resistance of the microstrip patch and result in lower efficiency.

In this paper, a new transparent antenna array is presented to serve as a sub-6 GHz 5G PC base station antenna with dual polarization. The single antenna element has a transparent radiator printed on a transparent glass laminate, which gives the proposed design the privilege of being partially invisible. This low visibility allows the proposed antenna to be feasibly integrated with other daily suitable surrounding equipment to achieve visual camouflage. In this paper, the street lamp is selected as an example of such surrounding equipment, which can be any other suitable one. A possible coverage scenario using the proposed PC base station is presented in Fig.3.

The antenna main concept has been introduced in [16]. Here, the antenna structure has slight changes to improve its performance, In addition, more illustrations about the antenna performance, fabrications and measurements have been included. The rest of the paper is divided into Section 2 which illustrates the proposed antenna design and its simulated and

measured results; Section 3 which discusses a 2×2 square antenna array configuration and its simulated and measured results; Section 4 which illustrates the integration of the antenna array with a street lamp and its effects on the antenna performance; and finally, the paper is concluded in Section 5.

2. The Proposed Antenna Element

Fig.4 presents an exploded view drawing of the proposed antenna. The antenna element shares similar features and working principles of our work proposed in [17] However, a major difference between the two antennas is that the proposed antenna element in this paper uses a transparent radiating layer.

The antenna consists of two layers separated by an air gap. The antenna radiates through a transparent layer made of glass (Layer A) with a size of $WS2 \times WS2 \times Hd2$. Two transparent square patches are printed on opposite sides of the glass laminate using a thin film of Indium Tin Oxide (ITO) to achieve optical transparency. The bottom patch (radiating patch) has a side length of $WP2$ while the top patch (parasitic patch) has a side length of $WP3$. Two perpendicular rectangular slots are cut in the radiating patch. Each slot is $L_Slot \times W_Slot$. The antenna is fed through a feeding layer (Layer B) made of a Rogers RT5880 laminate with a size of $WS1 \times WS1 \times Hd1$. A square copper patch (feeding patch) is printed on the top side of Layer B with a side length of $WP1$ while the bottom side has a ground plane of copper to support directional radiation. The feeding patch is fed by two 50Ω perpendicular feeding lines each of which is terminated by an RF connector for excitation. The two layers (Layer A and Layer B) are separated by an air gap with a height H using four supporting rods to, mechanically; fix the radiating layer above the feeding layer. The two layers, the patches and the slots are concentric and lie in the X-o-Y plane where their edges form angles of $\pm 45^\circ$ with the X and Y axes to provide the conventional dual-polarization of a base station antenna. It is worth noting that the glass laminate has a dielectric constant of 2.2 and a loss tangent of 0.0009 while the Rogers laminate has a dielectric constant of 2.3 and a tangential loss of 0.0054. The ITO film is $0.3 \mu\text{m}$ in thickness and has a conductivity of $5.6 \times 10^5 \text{ S/m}$ to achieve optical transparency of 88% [18]. The optimized dimensions (in mm) are determined as $WP1 = WP2 = 27$, $WP3 = 20$, $WS1 = 71$, $WS2 = 30$, $L_Slot = 9$, $W_Slot = 3$, $H = 7$, $Hd1 = 1.6$ and $Hd2 = 2.2$.

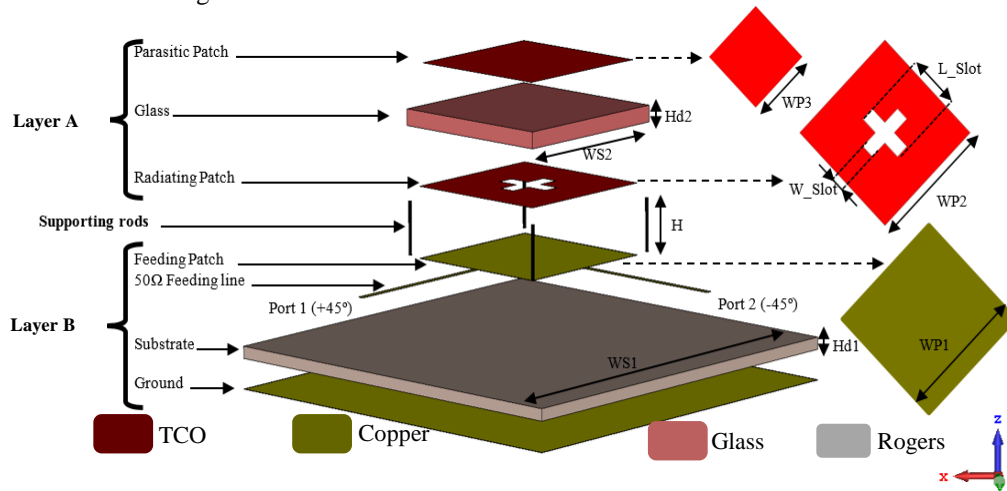


Fig.4. The exploded view drawing of the proposed antenna element.

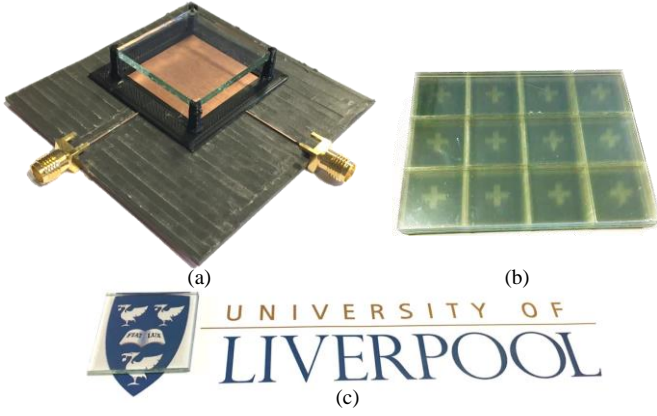


Fig. 5. Prototypes of (a) the proposed antenna element (b) 20 stacked radiating layers (c) a transparent single radiating layer.

When the antenna is excited through the RF connectors, the radiating layer is fed through the electric field coupling with the feeding layer. The function of the slots is to improve both the antenna impedance matching and transparency while the function of the parasitic patch is to add a capacitive loading to the input impedance of the antenna for further improvement of the impedance matching.

Fig.5(a) presents a model of the antenna element. In Fig.5(b), 20 stacked radiating layers are placed on a white paper to make the parasitic and radiating patches partially visible while Fig.5 (c) shows a single radiating layer with overall transparency of 77% (transparency for each patch is 88% while the transparency of the glass is around 99%).

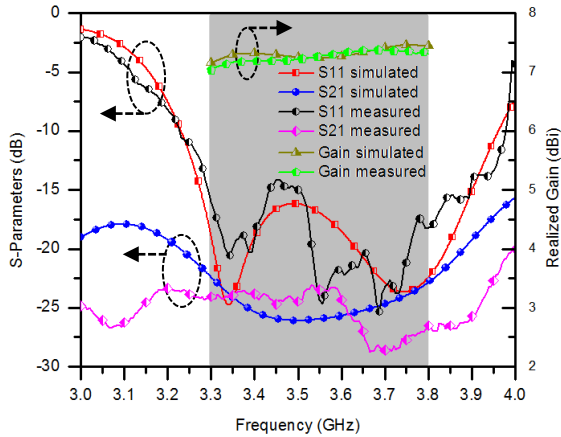


Fig. 6. Simulated and measured *S*-parameters, and realized gains.

Table 1. Comparison of previous work to the proposed design

Ref.	[19]	[20]	[21]	[22]	Proposed
Frequency Range (GHz)	3.5-5.1	3.3-3.6	3.45-3.55	3.65-3.81	3.3-3.8
Fractional BW	37.2%	8.7%	2.9%	4.3%	14.1%
Size (mm ³)	60×60×17	72×72×18.8	74×74×1.5	86×81×3	71×71×11
Coupling (dB)	-18	-28.8	-15	-31	-23
Gain (dBi)	8	8.2	8	10	7.3
Polarization	Dual	Dual	Single	Dual	Dual
PP (dB)	NA	24	NA	23	23
Camouflage	NA	NA	NA	NA	Available

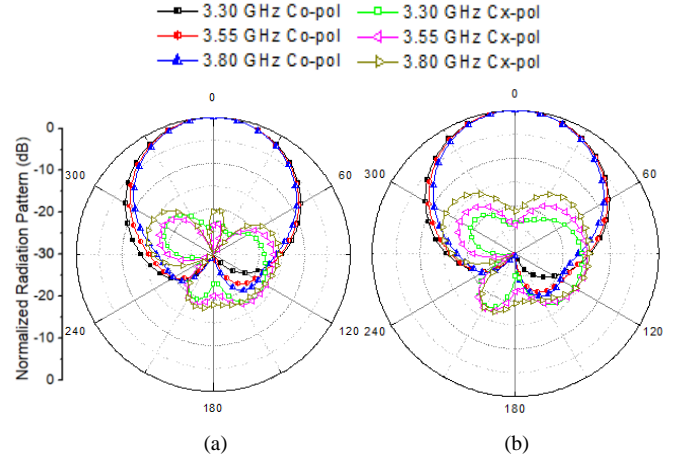


Fig. 7. Measured radiation patterns of proposed antenna element across (a) H-plane. (b) V-plane.

Fig.6 shows the antenna simulated and measured *S*-parameters. It is noticed that the antenna can cover the frequency range from 3.3-3.8 GHz with a reflection coefficient less than -15 dB and mutual coupling less than -23 dB. The simulated and measured gains are also plotted in Fig.6. As seen, the antenna measured gain is around 7.3 dBi over the working frequency range.

Fig.7 presents the measured radiation patterns in horizontal (X-o-Z) and vertical (Y-o-Z) planes at 3.3, 3.55 and 3.8 GHz for both co-polarized and cross-polarized radiations respectively. It is evident that the antenna has stable radiation patterns with half power beam widths (HPBW) of about 75° over the working frequency range. Also, the antenna enjoys polarization purity (PP) higher than 23 dB on boresight.

Table 1 illustrates a detailed comparison between our proposed design and previous designs which operate over similar frequency ranges. It is clear that the antenna proposed in this paper not only has a wide bandwidth (BW) and a small size but also enjoys small port-to-port coupling and high PP.

The proposed antenna gain is slightly less than the gains of the other reported design as the efficiency of the proposed antenna is around 72% - 74% (~ -1.4 dB). This is due to using ITO as a conductor, which has less conductivity than the copper used in the reported designs.

The privilege in the proposed antenna is its availability to be integrated with an object (such as a streetlamp in our case) for camouflage purposes because of its transparent radiating part.

3. A 2 × 2 Antenna Array

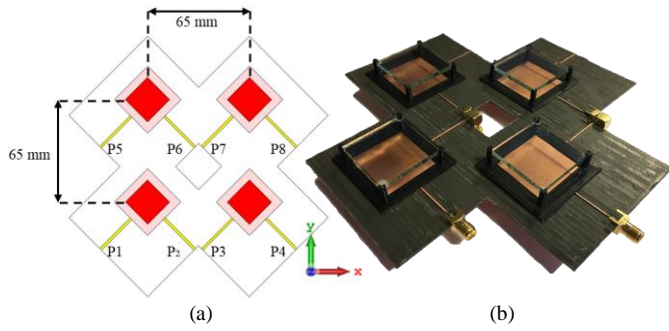


Fig.8. A 2 × 2 antenna array (a) layout (b) prototype.

To increase the antenna gain, a square 2 × 2 antenna array is formed as shown in Fig.8 (a) and a model has been fabricated as shown in Fig.8 (b). The spacing between any two adjacent elements is set to 65 mm ($0.8\lambda_0$ where λ_0 is the free space wavelength at the central frequency).

S-parameters for the ports (P1, P2... P8) of the antenna array are shown in Fig.9. The results indicate a 15 dB return loss across the desired BW from 3.3 to 3.8 GHz (while other ports are terminated by 50Ω loads) and worst-case mutual coupling of -23 dB between any pair of ports. It worth noting that the return losses of the feeding ports are identical due to the symmetry of the feeding structure. The average realized gain is 13.7 dBi as noticed from Fig.9.

The simulated and measured radiation patterns of the antenna array at the 3.3, 3.55 and 3.8 GHz are shown in Fig.10. The HPBW is 33° in both horizontal and vertical planes.

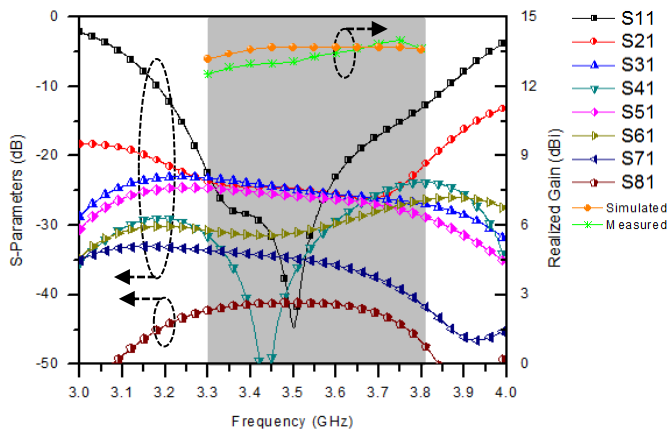


Fig.9. S-parameters and realized gains of the antenna array.

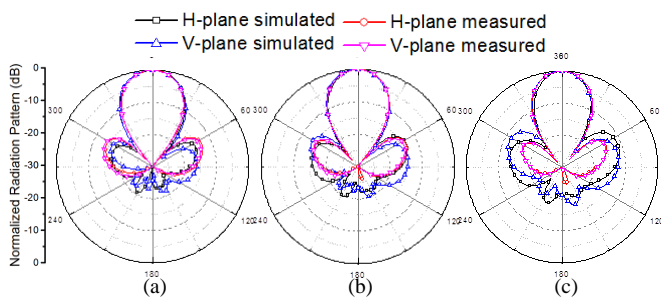


Fig.10. The simulated and measured radiation patterns of the array at (a) 3.3 GHz (b) 3.55 GHz (c) 3.8 GHz.

4. Integrated Antenna Array with a Street Lamp

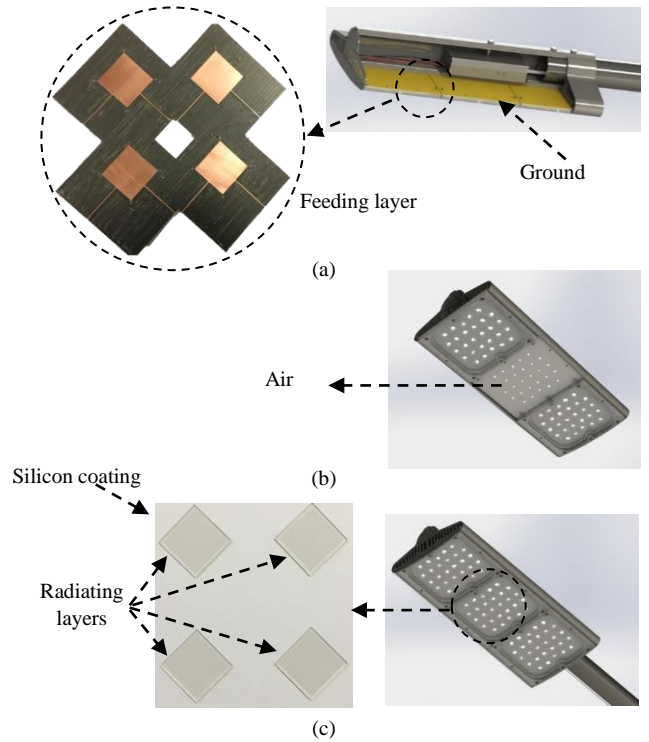


Fig.11. Integration of the proposed antenna array with a street lamp (a) feeding layer (b) air gap (c) radiating layers.

To achieve camouflage, the proposed antenna array is integrated into the head of a street lamp. The transparent radiating layer is integrated with the transparent glass cover of the head of the street lamp while the feeding layer is embedded inside the head as shown in Fig.11. The two layers are separated by a 7 mm air gap. Finally, a transparent thin protective silicon coating is placed on top of the radiating layer to provide protection to the antenna array.

To study the effect of the street lamp on the antenna performance, the antenna array was re-simulated after integration with the head of the street lamp using CST Microwave studio. Fig.12 shows the 3D radiation pattern in this case. It is clear that the antenna realized gain has slightly decreased to be 13.2 dBi due to the effect of the large size of the head of the street lamp and the silicon coating.

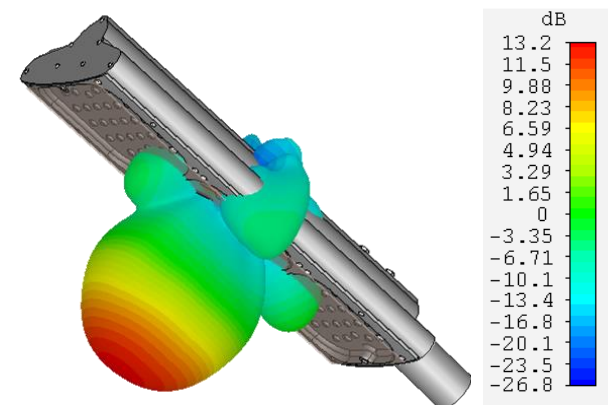


Fig.12. The simulated 3D radiation pattern of the proposed antenna array integrated with a street lamp.

5. Conclusions

To cope with the tradeoff between having good antenna performances and sufficient camouflage properties, this paper has proposed a new partially invisible antenna array for PC base stations working over 3.3 - 3.8 GHz. The antenna elements radiate through transparent patches formed using a thin film of a transparent ITO conductor printed on glass laminates to achieve 77% of visual transparency. All the electrical and radiation characteristics of the proposed antenna meet the requirements for 5G base station antennas. Moreover, being transparent, the antenna array has been successfully integrated into the head of a street lamp to achieve camouflage. Therefore, the proposed array is good enough to be employed as a camouflage 5G pico-cell base station.

6. References

- [1] R. Branson et al., "Creating a high efficiency, miniaturized power amplifier module for the emerging pico-cell base station market," *2014 IEEE Topical Conference on Power Amplifiers for Wireless and Radio Applications (PAWR)*, Newport Beach, CA, 2014, pp. 73-75.
- [2] L. H. Trinh, F. Ferrero, R. Staraj and J. Ribero, "700–960MHz MIMO antenna for Pico cell applications," *IEEE Antennas and Propagation Society International Symposium*, Orlando, FL, pp. 366-367, 2013.
- [3] Z. Chen, and K. Luk, *Antennas for Base Stations in Wireless Communications*, US: McGraw-Hill Professional, 2009.
- [4] J. Lebaric and Ah-Tuan Tan, "Ultra-wideband conformal helmet antenna," *Asia-Pacific Microwave Conference. Proceedings*, Sydney, NSW, Australia, pp. 1477-1481, 2000.
- [5] B. Sanz-Izquierdo, F. Huang and J. C. Batchelor, "Small size wearable button antenna," *First European Conference on Antennas and Propagation*, Nice, pp. 1-4, 2006.
- [6] M. Stanley, Y. Huang, H. Wang, H. Zhou, A. Alieldin, and S. Joseph, "A Transparent Dual-Polarized Antenna Array for 5G Smartphone Applications" *IEEE International Symposium on Antennas and Propagation & USNC/URSI National Radio Science Meeting*, Boston, USA, 2018.
- [7] N. Moghadasi and M. Koohestani, "A Simple UWB Microstrip-Fed Planar Rectangular Slot Monopole Antenna", *Loughborough Antenna & Propagation Conf.*, Loughborough, pp1-3, Nov. 2011.
- [8] P. Prajuabwan, S. Porntheeraphat, et. al, "ITO Thin Films prepared by Gas-Timing RF Magnetron Sputtering for Transparent Flexible Antenna", *Nano/Micro Engineered and Molecular Systems*, pp. 647 – 650, 2007.
- [9] R. Gordon, "Criteria for choosing transparent conductors", *MRS Bulletin*, Aug. 2000.
- [10] N. Guan, H. Furuya, D. Delaune and K. Ito, "Antennas made of transparent conductive films", *Propagation. In Electromagnetic. Research*, vol. 4, 2008.
- [11] T. Turpin, and R. Baktur, "Integrated solar meshed patch antennas", *IEEE Antennas and Wireless Propagation Letter*, vol. 8, pp. 693-696, 2009.
- [12] N. Outleb, J. Pinel, M. Drissi, and O. Bonnaud, "Microwave planar antenna with RF-sputtered indium tin oxide films", *Microwave and Optical. Technology. Lett.*, vol. 24, 2000.
- [13] M. Bourry, et.al, "Novel ITO alloy for microwave and optical applications", *Midwest Sym. on Circuits and Systems*, 615-618, August 2015.
- [14] H. J. Song, et. al, "A method for improving the efficiency of transparent film antennas", *IEEE Antennas and Wireless Propagation. Letter.* vol. 7, 2008.
- [15] A. Porch, et. al, "Electromagnetic absorption in transparent conducting films" *Jour. of Applied Physics.*, vol. 95, no. 9, May 2004.
- [16] A. Alieldin et al., "A Camouflage Antenna Array Integrated with a Street Lamp for 5G Picocell Base Stations," *13th European Conference on Antennas and Propagation (EuCAP)*, Krakow, Poland, pp. 1-4, 2019.
- [17] A. Alieldin, Y. Huang, M. Stanley, S. D. Joseph and D. Lei, "A 5G MIMO Antenna for Broadcast and Traffic Communication Topologies Based on Pseudo Inverse Synthesis," *IEEE Access*, vol. 6, pp. 65935-65944, 2018.
- [18] K. Narasimha Rao, "Optical and electrical properties of indium tin oxide films", *Indian journal of pure and applied physics*, vol 42, March 2004.
- [19] Y. Li, C. Wang, H. Yuan, N. Liu, H. Zhao and X. Li, "A 5G MIMO Antenna Manufactured by 3-D Printing Method," *IEEE Antennas and Wireless Propagation Letters*, vol. 16, pp. 657-660, 2017.
- [20] H. Huang, X. Li and Y. Liu, "5G MIMO Antenna Based on Vector Synthetic Mechanism," *IEEE Antennas and Wireless Propagation Letters*, vol. 17, no. 6, pp. 1052-1055, June 2018.
- [21] M. A. Al-Tarifi, M. S. Sharawi and A. Shamim, "Massive MIMO antenna system for 5G base stations with directive ports and switched beam steering capabilities," *IET Microwaves, Antennas & Propagation*, vol. 12, no. 10, pp. 1709-1718, 2018.
- [22] Y. Gao, R. Ma, Y. Wang, Q. Zhang and C. Parini, "Stacked Patch Antenna With Dual-Polarization and Low Mutual Coupling for Massive MIMO," *IEEE Transactions on Ant. and Propag.*, vol. 64, no. 10, pp. 4544-4549, Oct. 2016.